

$N\pi$ -excited state contamination in nucleon 3-point functions using ChPT

Oliver Bär*

Institut für Physik, Humboldt Universität zu Berlin

Newtonstraße 15, D-12489 Berlin, Germany

E-mail: obaer@physik.hu-berlin.de

The $N\pi$ -state contribution to nucleon 3-pt functions involving the pseudoscalar density $P(x)$ and the time component $A_4(x)$ of the axial vector current are computed to LO in ChPT. In case of the latter the $N\pi$ contribution is $O(M_N)$ enhanced compared to the single-nucleon ground state contribution. In addition, a relative sign in two terms of the $N\pi$ contribution leads an almost linear dependence on the operator insertion time, as it is observed in lattice data. In case of the pseudoscalar density the $N\pi$ contribution is strongly dependent on the momentum transfer, leading to a distortion of the pseudoscalar nucleon form factor. Finally, the $N\pi$ state contamination in the form factors result in a violation of the generalized Goldberger-Treiman relation as observed in various lattice calculations.

*The 37th Annual International Symposium on Lattice Field Theory - LATTICE 2019
June 16-22 2019, Wuhan, China.*

*Speaker.

1. Introduction

While physical point simulations eliminate the need for a chiral extrapolation of lattice data, some problems become more severe with the pions as light as in Nature. The signal-to-noise problem [1, 2] typically becomes more pronounced the smaller the pion mass is, limiting the euclidean time separations in the correlation functions measured in lattice simulations. At the same time the excited-state contamination due to multi-particle states involving light pions gets larger since the gap to the single-particle ground state shrinks with smaller pion mass.

In a series of papers [3, 4, 5] baryon chiral perturbation theory (ChPT) [6] has been employed to estimate the two-particle nucleon-pion ($N\pi$) state contamination in lattice estimates of the nucleon mass, nucleon charges and pdf moments.¹ The size of this particular excited-state contamination depends on the quantity one is looking at. As shown at last year's lattice conference [9] the induced pseudoscalar form factor \tilde{G}_P of the nucleon is particularly prone to an $N\pi$ -state contamination. ChPT predicts that the lattice plateau estimate for this form factor systematically underestimates the physical form factor. This bias is momentum transfer dependent, the smaller Q^2 the larger the underestimation. As a result the lattice data show a flatter Q^2 dependence than the pion-pole-dominance (PPD) model suggests. Using the ChPT result to correct data from the PACS collaboration [10] good agreement with the PPD model and experimental data is achieved.

In the following new results are presented for the $N\pi$ contamination in (i) the nucleon 3-point (pt) function involving the temporal component $A_4(x)$ of the axial vector current and (ii) lattice estimates of the pseudoscalar form factor G_P . In addition, with the results for the two axial form factors we explicitly check for the role the $N\pi$ contamination plays in the violation of the generalized Goldberger-Treiman relation observed in various lattice calculations [11, 12, 13]. Technical details and a full account of the results are given in [14, 15].

2. $N\pi$ state contribution in nucleon axial and pseudoscalar form factors

The isovector nucleon axial form factors are defined by the matrix element of the local isovector axial vector current between single nucleon states,

$$\langle N(\vec{p}', s') | A_\mu^a(0) | N(\vec{p}, s) \rangle = \bar{u}(p', s') \left(\gamma_\mu \gamma_5 G_A(Q^2) - i \gamma_5 \frac{Q_\mu}{2M_N} \tilde{G}_P(Q^2) \right) \frac{\sigma^a}{2} u(p, s). \quad (2.1)$$

The nucleon momenta \vec{p}, \vec{p}' in the initial and final state imply the euclidean 4-momentum transfer $Q_\mu = (iE_{\vec{p}'} - iE_{\vec{p}}, \vec{q})$, $\vec{q} = \vec{p}' - \vec{p}$. We follow the kinematic setup $\vec{p}' = 0$ that is often chosen in numerical simulations. $G_A(Q^2)$ and $\tilde{G}_P(Q^2)$ on the right hand side of (2.1) refer to the axial and induced pseudoscalar form factors, respectively. Analogously, the matrix element of the local isovector pseudoscalar density $P^a(x)$ defines the pseudoscalar form factor,

$$m_q \langle N(p', s') | P^a(0) | N(p, s) \rangle = m_q G_P(Q^2) \bar{u}(p', s') \gamma_5 \frac{\sigma^a}{2} u(p, s). \quad (2.2)$$

Lattice calculations of the form factors follow a standard procedure. It is based on the calculation of the nucleon 2-pt function and the nucleon 3-pt functions involving the axial vector current and

¹For reviews see Refs. [7, 8].

pseudoscalar density, and the ratio of these correlation functions,

$$R_\mu(\vec{q}, t, t') = \frac{C_{3,X_\mu}(\vec{q}, t, t')}{C_2(0, t)} \sqrt{\frac{C_2(\vec{q}, t - t')}{C_2(0, t - t')} \frac{C_2(\vec{0}, t)}{C_2(\vec{q}, t)} \frac{C_2(\vec{0}, t')}{C_2(\vec{q}, t')}}}, \quad \mu = 1, \dots, 4, P. \quad (2.3)$$

$\mu = 1, \dots, 4$ refers to the ratio with the axial vector current 3-pt function, and $\mu = P$ to the case with the pseudoscalar density. The euclidean times t and t' denote the source-sink separation and the operator insertion time, respectively. The ratios are defined such that, in the asymptotic limit $t, t', t - t' \rightarrow \infty$, they converge to constant asymptotic values $R_\mu(\vec{q}, t, t') \rightarrow \Pi_\mu(\vec{q})$. These are related to the form factors according to ($E_{N,\vec{q}}$: energy of a nucleon with momentum \vec{q})

$$\Pi_k(\vec{q}) = \frac{i}{\sqrt{2E_{N,\vec{q}}(M_N + E_{N,\vec{q}})}} \left((M_N + E_{N,\vec{q}}) G_A(Q^2) \delta_{3k} - \frac{\tilde{G}_P(Q^2)}{2M_N} q_3 q_k \right), \quad (2.4)$$

$$\Pi_4(\vec{q}) = \frac{q_3}{\sqrt{2E_{N,\vec{q}}(M_N + E_{N,\vec{q}})}} \left(G_A(Q^2) + \frac{M_N - E_{N,\vec{q}}}{2M_N} \tilde{G}_P(Q^2) \right), \quad (2.5)$$

$$\Pi_P(\vec{q}) = \frac{q_3}{\sqrt{2E_{N,\vec{q}}(M_N + E_{N,\vec{q}})}} G_P(Q^2). \quad (2.6)$$

The form factors are easily obtained from these expressions. In practice one only has access to the ratios $R_\mu(\vec{q}, t, t')$ at time separations t, t' far from being asymptotically large. In that case the correlation functions and the ratios contain a contribution from excited states with the same quantum numbers as the nucleon. Instead of the true form factors one is interested in one obtains *effective* form factors including an excited-state contamination,²

$$G_X^{\text{eff}}(Q^2, t, t') = G_X(Q^2) \left[1 + \varepsilon_X(Q^2, t, t') \right], \quad X = A, P, \tilde{P}. \quad (2.7)$$

The excited-state contribution $\varepsilon_X(Q^2, t, t')$ vanishes for $t, t', t - t' \rightarrow \infty$.

The dominant excited-state contamination for physical pion mass and large time separations is due to two-particle $N\pi$ states. It can be computed in ChPT, the low-energy effective theory of QCD [16]. Working at leading order (LO) in SU(2) baryon ChPT this theory contains a nucleon doublet with the proton and neutron fields and the three mass degenerate pions (we assume isospin symmetry). There is a single interaction vertex which implies the well-known one-pion-exchange-potential between a pair of nucleons. At LO only a few low-energy coefficients (LECs) enter: the axial charge and the pion decay constant as well as the pion and nucleon masses. The $N\pi$ contribution to the 2-pt and 3-pt functions and the ratio R_μ are straightforwardly computed, yielding explicit expressions for the $N\pi$ contamination $\varepsilon_X(Q^2, t, t')$. Using the known phenomenological values for the LECs ChPT makes predictions for the $N\pi$ -state contamination present in lattice calculations of the form factors.

3. Axial vector 3-pt function with temporal component A_4

In principle lattice data for the 3-pt function involving the temporal component A_4 and the associated ratio R_4 may be used in the calculation of the axial form factors, see eq. (2.5). In

²For brevity we introduce the notation $G_{\tilde{P}} = \tilde{G}_P$.

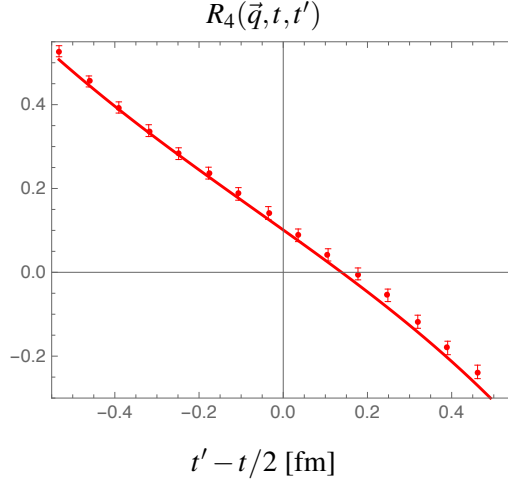


Figure 1: RQCD data [11] for the correlation function ratio $R_4(\vec{q}, t, t')$ (red data points) for $t = 1.06$ fm and the ChPT result (red line) [14].

practice, however, the data are usually excluded for large statistical errors and because of a large excited-state contamination. Examples for $R_4(\vec{q}, t, t')$ data can be found in [11, 17], and also in Y.-C. Jang’s contribution to this conference [18]. The ratio $R_4(\vec{q}, t, t')$ shows, for fixed \vec{q} and t , a nearly linear dependence on the operator insertion time t' . In contrast to the other ratios there does not exist a plateau estimate. Thus, it is not obvious how to extract the single-nucleon (SN) state contribution.

In ChPT the 3-pt function is the sum of the SN and the $N\pi$ contribution,

$$C_{3,\mu=4}(\vec{q}, t, t') = C_{3,\mu=4}^N(\vec{q}, t, t') + C_{3,\mu=4}^{N\pi}(\vec{q}, t, t'). \quad (3.1)$$

If we perform the non-relativistic expansion for the nucleon energy, $E_{N,\vec{q}} \approx M_N + \vec{q}^2/2M_N$, we find

$$C_{3,\mu=4}^N = \mathcal{O}(M_N^{-1}), \quad C_{3,\mu=4}^{N\pi} = \mathcal{O}(1). \quad (3.2)$$

Thus, the $N\pi$ contribution in (3.1) is “ $\mathcal{O}(M_N)$ -enhanced” compared to the SN contribution, explaining the large excited-state contamination usually observed in lattice data for this correlation function. The origin of the large $N\pi$ contribution is that the axial vector current can either directly create a pion at t' that propagates to the sink where it is annihilated. Or a pion, created at the source, is destroyed by the axial vector current at t' . It turns out [14] that there is a relative sign between these two large contributions. As a consequence, $R_4(\vec{q}, t, t')$ displays a $\sinh[E_{\pi,\vec{q}}(t' - t/2)]$ behavior, explaining the observed nearly linear dependence on t' .

Figure 1 shows the data of the RQCD collaboration [11] for $R_4(\vec{q}, t, t')$ (red data points) as a function of the (shifted) operator insertion time $t' - t/2$ for fixed $t = 1.07$ fm and for \vec{q} corresponding to a momentum transfer $Q^2 = 0.073$ GeV². The LO ChPT result for the ratio is shown by the red line. We emphasize that the ChPT result is not a fit to the lattice data, all LECs are fixed by their phenomenological values.

Apparently, ChPT describes the data very well, in fact better than expected. The time separations $t - t'$ and t' need to be sufficiently large such that pion physics dominates the 3-pt function,

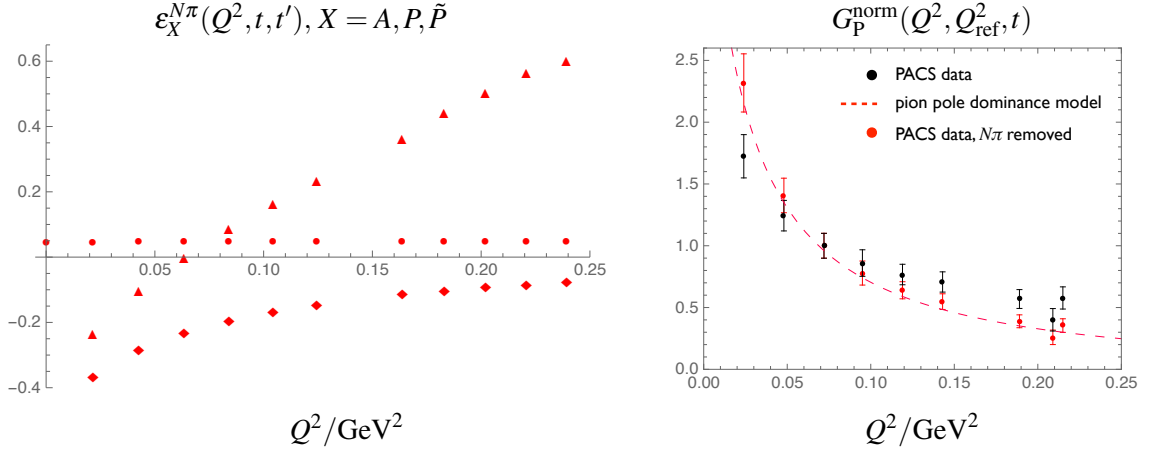


Figure 2: Left panel: The relative deviations $\varepsilon_A(Q^2, t, t')$ (circles), $\varepsilon_P(Q^2, t, t')$ (diamonds) and $\varepsilon_{\tilde{P}}(Q^2, t, t')$ (triangles) as a function of Q^2 for $t = 2$ fm and $t' = t/2$. Discrete Q^2 values for finite spatial volumes satisfying $M_\pi L = 6$. Right panel: PACS data from [10] for the normalized pseudoscalar form factor $G_P^{\text{norm}}(Q^2, Q_{\text{ref}}^2, t)$ (black) for $t = 1.3$ fm and $Q_{\text{ref}}^2 = 0.072 \text{ GeV}^2$. Red symbols show the data with the $N\pi$ contamination removed. The dashed red line corresponds to the PPD result.

and we can naively expect a minimal separation of about 1 fm for both $t - t'$ and t' . Therefore, for a source-sink separation as small as $t \approx 1$ fm we may expect ChPT to describe the 3-pt function and the ratio for t' close to $t/2$, if at all. The good agreement for all t' , even close to source and sink, is surprising and deserves further study.

4. Pseudoscalar form factor

As a measure for the $N\pi$ -state contribution we introduce the relative deviation of the effective form factor from the true form factors,

$$\varepsilon_X^{N\pi}(Q^2, t, t') \equiv \frac{G_P^{\text{eff}}(Q^2, t, t')}{G_P(Q^2)} - 1, \quad X = A, \tilde{P}, P. \quad (4.1)$$

The left panel in figure 2 shows $\varepsilon_X^{N\pi}$ for all three form factors. The source-sink separation is chosen $t = 2$ fm and $t' = t/2$, corresponding to the so-called mid-point estimate for the form factors. The discrete values for the momentum transfer correspond to the lowest possible values for spatial volumes with $M_\pi L = 6$, as it is realized in the lattice simulations of the PACS collaboration [10], for example. The results for the axial form factors (dots and diamonds) have already been presented in [9], new are the results for the pseudoscalar form factor (triangles). Figure 2 shows that the bias of the mid-point estimate G_P^{mid} is momentum dependent: G_P^{mid} underestimates for $Q^2 \lesssim 0.06 \text{ GeV}^2$ (up to $\approx -20\%$ for the smallest momentum transfer), and overestimates for $Q^2 \gtrsim 0.06 \text{ GeV}^2$ (up to $\approx +50\%$ for the largest momentum transfer in the figure).

To compare with lattice data it is useful to consider the normalized pseudoscalar form factor

$$G_P^{\text{norm}}(Q^2, Q_{\text{ref}}^2, t) \equiv \frac{G_P^{\text{plat}}(Q^2, t)}{G_P^{\text{plat}}(Q_{\text{ref}}^2, t)}, \quad (4.2)$$

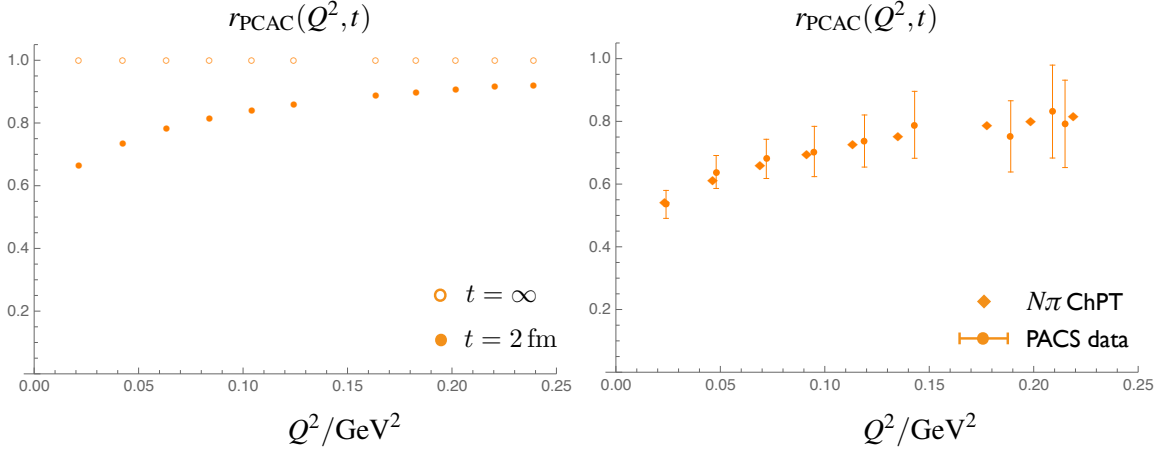


Figure 3: Left panel: LO ChPT result for $r_{\text{PCAC}}(Q^2, t)$ for $t = 2 \text{ fm}$ (solid symbols) and $t = \infty$ (open symbols). Right panel: $r_{\text{PCAC}}(Q^2, t)$, ChPT result (diamonds) compared to PACS data (dots).

which is independent of Z_P . The right panel in figure 2 shows PACS lattice data [] for this ratio (black symbols) for $Q_{\text{ref}}^2 = 0.072(2) \text{ GeV}^2$. The red dashed line shows the PPD result for this ratio. Even though the statistical errors are large the momentum transfer dependence of the lattice data displays a flatter Q^2 dependence than the PPD model, just as ChPT predicts for the impact of the $N\pi$ state contamination. With the ChPT result we can analytically remove the anticipated LO $N\pi$ -state contamination from the lattice data. The result is shown by the red data points in fig. 2, which show much better agreement with the PPD model. The good agreement is again surprising, given that the lattice data is obtained with a fairly short source-sink separation $t \approx 1.3 \text{ fm}$.

5. Generalized Goldberger-Treiman relation

The two axial and the pseudoscalar form factor are not independent. The partially conserved axial vector current (PCAC) relation, $\partial_\mu A_\mu^a(x) = 2m_q P^a(x)$, taken between SN states, leads to the so-called generalized Goldberger-Treiman (GGT) relation

$$2M_N G_A(Q^2) - \frac{Q^2}{2M_N} \tilde{G}_P(Q^2) = 2m_q G_P(Q^2) \quad (5.1)$$

between the three form factors. This relation, however, is usually found to be violated by lattice estimates for the form factors. As a measure for this violation one may define the ratio

$$r_{\text{PCAC}}(Q^2, t) = \frac{Q^2}{4M_N^2} \frac{\tilde{G}_P^{\text{eff}}(Q^2, t, t/2)}{G_A^{\text{eff}}(Q^2, t, t/2)} + \frac{2m_q}{2M_N} \frac{G_P^{\text{eff}}(Q^2, t, t/2)}{G_A^{\text{eff}}(Q^2, t, t/2)}. \quad (5.2)$$

If the effective form factors are equal to the physical ones r_{PCAC} is independent of the momentum transfer and equals 1. In practice, however, one typically finds a Q^2 dependent r_{PCAC} smaller than 1. The smaller the momentum transfer the larger the deviation from 1, see Refs. [11, 12, 13] and the plenary talk by T. Bhattacharya at this conference [19].

Having the ChPT results for the $N\pi$ -state contamination in all three form factor estimates we compute r_{PCAC} and check for the role of $N\pi$ states in the violation of the gGT relation. The

left panel of fig. 3 shows the ChPT results for $t = 2$ fm and $t = \infty$ (the discrete values for the momentum transfer are again the lowest ones associated with $M_\pi L = 6$). We find that ChPT predicts $r_{\text{PCAC}}(Q^2, t = 2 \text{ fm}) < 1$ with the deviation increasing the smaller Q^2 is, just as it is found in lattice simulations. The right panel of fig. 3 displays the ChPT result for smaller source-sink separation $t = 1.3$ fm, together with r_{PCAC} formed with the lattice results of the PACS collaboration in [10] obtained at approximately this t . We observe good agreement with the data. The dominant source for $r_{\text{PCAC}} < 1$ can be traced back to the large $N\pi$ contamination in the induced pseudoscalar form factor and the underestimation of $\tilde{G}_P(Q^2, t)$, see fig. 2, left panel.

6. Conclusions

The ChPT results strongly suggest that many observed deviations between lattice estimates and experimental form factor results are due to the $N\pi$ -state contamination, for instance the violation of the generalized Goldberger-Treiman relation.

References

- [1] G. Parisi, Phys. Rept. **103** (1984) 203.
- [2] G. P. Lepage, The Analysis of Algorithms for Lattice Field Theory, in *Boulder ASI 1989:97-120*, pp. 97–120, 1989.
- [3] O. Bär, Phys. Rev. **D92** (2015) 074504.
- [4] O. Bär, Phys. Rev. **D94** (2016) 054505.
- [5] O. Bär, Phys. Rev. **D95** (2017) 034506.
- [6] T. Becher and H. Leutwyler, Eur. Phys. J. **C9** (1999) 643.
- [7] O. Bär, Int. J. Mod. Phys. **A32** (2017) 1730011.
- [8] O. Bär, EPJ Web Conf. **175** (2018) 01007.
- [9] O. Bär, PoS **LATTICE2018** (2018) 061.
- [10] K.-I. Ishikawa *et al.*, Phys. Rev. **D98** (2018) 074510.
- [11] G. S. Bali *et al.*, Phys. Lett. **B789** (2019) 666.
- [12] R. Gupta *et al.*, Phys. Rev. **D96** (2017) 114503.
- [13] Y.-C. Jang *et al.*, EPJ Web Conf. **175** (2018) 06033.
- [14] O. Bär, Phys. Rev. **D99** (2019) 054506.
- [15] O. Bär, arXiv:1906.03652 [hep-lat], submitted to PRD.
- [16] B. C. Tiburzi, Phys. Rev. **D80** (2009) 014002.
- [17] T. Schulz, *A new method for suppressing excited-state contaminations on the nucleon form factors*. Talk given at 36th Symposium on Lattice Field Theory, East Lansing, Michigan, U.S.A. <https://indico.fnal.gov/event/15949/session/13/contribution/118>.
- [18] Y.-C. Jang, *Nucleon Axial and Electromagnetic Form Factors from 2+1+1-flavor QCD*. Talk given at this conference, <https://indico.cern.ch/event/764552/contributions/3420558/>.
- [19] T. Bhattacharya, *Review of results of recent nucleon structure & matrix element calculations*. Talk given at this conference. <https://indico.cern.ch/event/764552/contributions/3420543/>.